

Alma Mater Studiorum Università di Bologna  
Archivio istituzionale della ricerca

Improved centrifugal and hyperfine analysis of ND<sub>2</sub>H and NH<sub>2</sub>D and its application to the spectral line survey of L1544

This is the final peer-reviewed author's accepted manuscript (postprint) of the following publication:

*Published Version:*

Melosso M., Bizzocchi L., Dore L., Kisiel Z., Jiang N., Spezzano S., et al. (2021). Improved centrifugal and hyperfine analysis of ND<sub>2</sub>H and NH<sub>2</sub>D and its application to the spectral line survey of L1544. JOURNAL OF MOLECULAR SPECTROSCOPY, 377, 111431-1-111431-8 [10.1016/j.jms.2021.111431].

*Availability:*

This version is available at: <https://hdl.handle.net/11585/867650> since: 2022-02-24

*Published:*

DOI: <http://doi.org/10.1016/j.jms.2021.111431>

*Terms of use:*

Some rights reserved. The terms and conditions for the reuse of this version of the manuscript are specified in the publishing policy. For all terms of use and more information see the publisher's website.

This item was downloaded from IRIS Università di Bologna (<https://cris.unibo.it/>).  
When citing, please refer to the published version.

(Article begins on next page)

This is the final peer-reviewed accepted manuscript of:

**M. Melosso, L. Bizzocchi, L. Dore, Z. Kisiel, N. Jiang, S. Spezzano, P. Caselli, J. Gauss, C. Puzzarini. Improved centrifugal and hyperfine analysis of ND<sub>2</sub>H and NH<sub>2</sub>D and its application to the spectral line survey of L1544. J. Mol. Spectrosc. 377 (2021) 111431**

The final published version is available online at:

<https://doi.org/10.1016/j.jms.2021.111431>

#### Terms of use:

Some rights reserved. The terms and conditions for the reuse of this version of the manuscript are specified in the publishing policy. For all terms of use and more information see the publisher's website.

*This item was downloaded from IRIS Università di Bologna (<https://cris.unibo.it/>)*

***When citing, please refer to the published version.***

# Improved centrifugal and hyperfine analysis of ND<sub>2</sub>H and NH<sub>2</sub>D and its application to the spectral line survey of L1544

Mattia Melosso<sup>a,\*</sup>, Luca Bizzocchi<sup>b</sup>, Luca Dore<sup>a</sup>, Zbigniew Kisiel<sup>c</sup>, Ningjing Jiang<sup>a</sup>, Silvia Spezzano<sup>b</sup>, Paola Caselli<sup>b</sup>, Jürgen Gauss<sup>d</sup>, Cristina Puzzarini<sup>a,\*</sup>

<sup>a</sup>*Dipartimento di Chimica “Giacomo Ciamician”, Università di Bologna, Via F. Selmi 2, 40126 Bologna, Italy*

<sup>b</sup>*Center for Astrochemical Studies, Max Planck Institut für extraterrestrische Physik, Gießenbachstraße 1, 85748 Garching bei München, Germany*

<sup>c</sup>*Institute of Physics, Polish Academy of Sciences, Al. Lotników 32/46, 02-668 Warszawa, Poland*

<sup>d</sup>*Department Chemie, Johannes Gutenberg-Universität Mainz, Duesbergweg 10-14, 55128 Mainz, Germany*

---

## Abstract

Quantifying molecular abundances of astrochemical species is a key step towards the understanding of the chemistry occurring in the interstellar medium. This process requires a profound knowledge of the molecular energy levels, including their structure resulting from weak interactions between nuclear spins and the molecular rotation. With the aim of increasing the quality of spectral line catalogs for the singly- and doubly-deuterated ammonia (NH<sub>2</sub>D and ND<sub>2</sub>H), we have revised their rotational spectra by observing many hyperfine-resolved lines and more accurate high-frequency transitions. The measurements have been performed in the submillimeter-wave region (265–1565 GHz) using a frequency modulation submillimeter spectrometer and in the far-infrared domain (45–220 cm<sup>-1</sup>) with a synchrotron-based Fourier-transform interferometer. The analysis of the new data, with the interpretation of the hyperfine structure supported by state-of-the-art quantum-chemical calculations, led to an overall improvement of all spectroscopic parameters. Moreover, the effect of the inclusion of deuterium splittings in the analysis of astrophysical NH<sub>2</sub>D emissions at millimeter wavelengths has been tested using recent observations of the starless core L1544, an ideal astrophysical laboratory for the study of deuterated species. Our results show that accounting for hyperfine interactions leads to a small but significant change in the physical parameters used to model NH<sub>2</sub>D line emissions.

**Keywords:** Ammonia, Hyperfine structure, Rotational spectroscopy, Interstellar medium, Deuterium fractionation, Starless core

---

## 1. Introduction

The increasing sensitivity and spectral resolution of modern radio-telescopes are stimulating a large number of laboratory studies that aim at supporting astronomical observations of molecules in the Interstellar Medium (ISM). On the one hand, these studies mostly exploit rotational spectroscopy techniques to characterize small- to medium-sized species, the reason being that rotational signatures can undoubtedly prove (and quantify) the presence

of a molecule in the ISM [1]. On the other hand, laboratory efforts on a particular molecular system can be motivated by several aspects. Among them, the search for pre-biotic species and molecules that are more generally related to the origin of life is still one of the hottest topics in astrochemistry [2, 3, 4], although any attempt to detect amino acids in the gas-phase has so far remained unsuccessful [5, 6]. However, being evident that the ISM exhibits a complex chemistry, the characterization of new Complex Organic Molecules (COMs, i.e. species containing at least six atoms and composed of carbon, hydrogen, oxygen and/or nitrogen) is the main theme of joint laboratory-observational studies [7, 8, 9, 10]. Moreover, the new detections of

---

\*Corresponding authors

Email addresses: mattia.melosso2@unibo.it (Mattia Melosso), cristina.puzzarini@unibo.it (Cristina Puzzarini)

ions [11], radicals [12], carbon-chains [13, 14], and rings [15] –including aromatic ones [16]– open new perspectives for an even richer molecular complexity.

All these aspects contribute to our understanding of the interstellar chemistry and are useful to probe excitation mechanisms and kinematics, as well as to trace the evolutionary stage of astronomical objects [17, 18] and their chemical differentiation [19, 20, 21]. However, the evaluation of molecular abundances, which are in turn the building-blocks of astrochemical models, is a crucial point that requires a deep knowledge of the molecule under investigation: this can include information about vibrational excited states [22, 23], a correct computation of partition function values [24], or the effect of nuclear electric and magnetic interactions giving raise to the so-called hyperfine structures (HFS).

Recently, the importance of such effects in the analysis of singly-deuterated ammonia ( $\text{NH}_2\text{D}$ ) line emission towards the starless core H-MM1 has been pointed out [25, 26] and, subsequently, addressed in our laboratory in Bologna [27]. In the context of a broader investigation of the rotational spectra of ammonia isotopologues, we have extended the centrifugal analysis of  $\text{NH}_2\text{D}$  and  $\text{ND}_2\text{H}$  at higher frequencies and measured additional hyperfine-resolved transitions, especially those of astronomical interest. The new measurements have been combined with literature data to obtain the best set of spectroscopic constants for both singly- and doubly-deuterated ammonia, in order to generate accurate line catalogs. Then, the effect of including deuterium hyperfine interactions on the analysis of astrophysical  $\text{NH}_2\text{D}$  emissions at millimeter wavelengths has been tested using recent observations of the low-mass star-forming core L1544.

The paper is organized as follows. First, the spectral features of the rotation-inversion spectrum of  $\text{ND}_2\text{H}$  compared to that of  $\text{NH}_2\text{D}$  (Section 2) are presented. Then, the submillimeter spectrometer and the synchrotron-based Fourier transform interferometer used for the measurements are described (Section 3). In Section 4, the results of our spectral analysis are given and applied to  $\text{NH}_2\text{D}$  line emissions towards the starless core L1544. Finally, our findings are summarized in Section 5.

## 2. Theory

The main features of the rotational spectrum of  $\text{NH}_2\text{D}$  have been exhaustively described in Melosso *et al.* ([27], hereafter **Paper I**). The spectroscopic behavior of  $\text{ND}_2\text{H}$  is quite similar to that of  $\text{NH}_2\text{D}$ ; therefore, we only briefly recall the key aspects and highlight the major differences.

Doubly-deuterated ammonia is an asymmetric-top rotor with a double-minima potential energy surface. The tunneling between the two equivalent configurations splits each  $J_{K_a, K_c}$  rotational level into two sub-levels, one symmetric (*s*) and one anti-symmetric (*a*) with respect to inversion. As in the case of  $\text{NH}_2\text{D}$ , the inversion motion of  $\text{ND}_2\text{H}$  occurs along the *c*-axis; however, the *a*- and *b*-axes are reversed. Hence, the spectrum of  $\text{ND}_2\text{H}$  is characterized by weak *b*-type transitions within each sub-state and stronger *c*-type transitions connecting the two inversion states [28].

All nuclei present in the molecule having nonzero nuclear spins contribute to the hyperfine structure of the rotational spectrum of  $\text{ND}_2\text{H}$ . The HFS is dominated by the nuclear quadrupole coupling (NQC) of nitrogen, but spin-rotation (SR) interactions as well as NQC effects due to the deuterium nuclei have an appreciable impact on it. Moreover, the presence of two equivalent D nuclei leads to the existence of *ortho* and *para* species, and the total nuclear spin  $I_{\text{D,tot}} = I_{\text{D}_1} + I_{\text{D}_2}$  must be taken into account. The *ortho* species corresponds to  $I_{\text{D,tot}} = 0$  or 2, whereas the *para* form is characterized by  $I_{\text{D,tot}} = 1$ . This results in an *ortho:para* spin-statistical weight ratio of 2:1. Since the two equivalent particles are bosons, the Bose-Einstein statistics holds. Given that the total wavefunction has to be symmetric with the respect to the exchange of the two D nuclei, the *ortho* form has rotation-inversion states of the type (*s, ee*), (*s, oo*), (*a, eo*), and (*a, oe*), while the *para* species possesses (*s, eo*), (*s, oe*), (*a, ee*), and (*a, oo*) states.

While the Hamiltonian used in the present analysis is identical to the one described in **Paper I**, the angular momentum coupling scheme adopted for the labelling of energy levels is slightly different:

$$\begin{aligned}\mathbf{F}_1 &= \mathbf{J} + \mathbf{I}_N, \\ \mathbf{F}_2 &= \mathbf{F}_1 + \mathbf{I}_{\text{D,tot}}, \\ \mathbf{F} &= \mathbf{F}_2 + \mathbf{I}_H,\end{aligned}\tag{1}$$

because of the presence of the two identical deuterium nuclei and only one hydrogen.

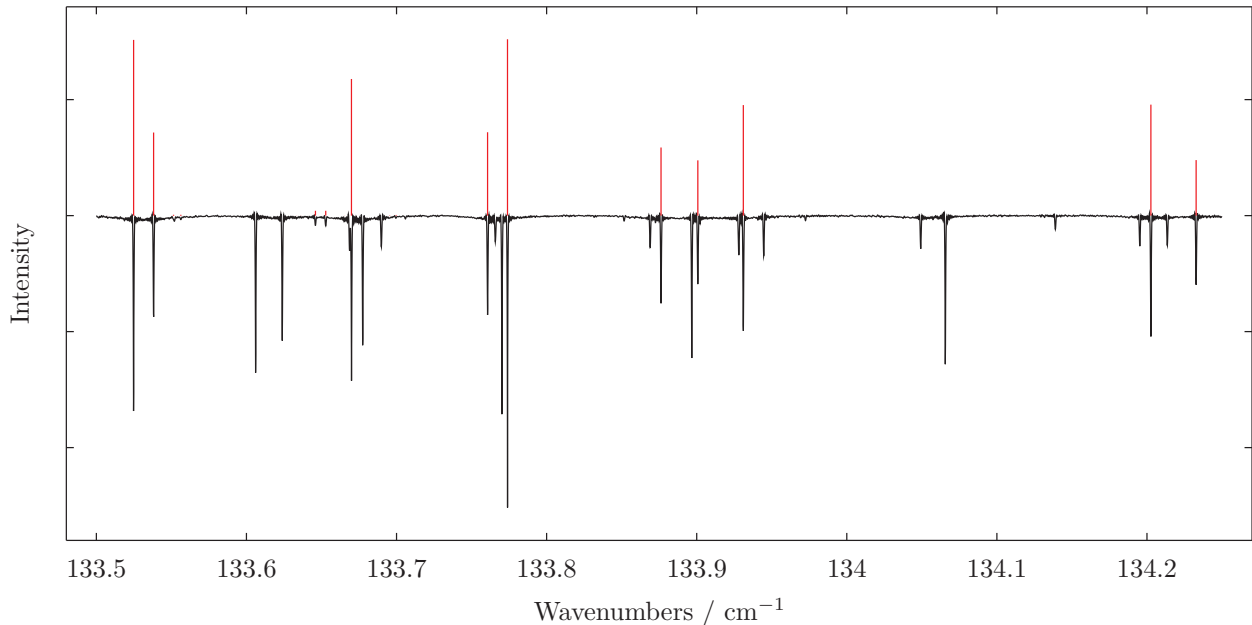


Figure 1: Portion of the FIR spectrum of ND<sub>2</sub>H (black trace). The red bars indicate the position and intensity of some *c*-type R branch transitions, as predicted using the spectroscopic constants determined in this work. The remaining spectral lines belong to ND<sub>3</sub> or to other by-products of the discharge. The intensity on the *y*-axis is expressed in arbitrary units.

### 3. Experiment

Rotational transitions of singly- and doubly-deuterated ammonia were recorded in the range 265–1565 GHz with a frequency-modulation sub-millimeter spectrometer [29]. The radiation source of the spectrometer is constituted by a series of Gunn diodes emitting between 80 and 134 GHz, which can be coupled with passive frequency multipliers (doublers and triplers). Terahertz frequencies are obtained by connecting two triplers in cascade guided by Gunn diodes working in the F band (115–134 GHz) [30, 31]. However, the twelfth harmonic of their radiation remains detectable with a power around few tens of  $\mu$ W, thus enabling to reach frequencies up to 1.6 THz. The radiation source is phase-locked to a harmonic of a centimeter-wave synthesizer (2–18 GHz), frequency modulated at  $f = 1 - 48$  kHz, and referenced to a 5 MHz rubidium atomic clock. The measurements were performed in a 3 m long glass absorption cell with the optical elements of the spectrometer arranged to perform, whenever possible, Lamb-dip measurements (for further details about the set-up, see **Paper I** as well as Refs. [32, 33, 34]). The output radiation was then detected by a liquid helium-cooled InSb bolometer and sent to a lock-in amplifier, set at twice the modulation frequency ( $2f$

detection scheme). Here, the sample of NH<sub>2</sub>D was produced using the same methodology employed in **Paper I** (a small flow of NH<sub>3</sub> in a cell where D<sub>2</sub> had been previously discharged), whereas a good yield of ND<sub>2</sub>H was obtained by flowing simply ND<sub>3</sub> into the absorption cell.

Additional transitions in the range 45–220  $\text{cm}^{-1}$  were observed at the SOLEIL synchrotron using a Bruker IFS125HR FTIR interferometer, whose source is the bright synchrotron radiation extracted by the AILES beamline. The far-infrared (FIR) spectrum was recorded at a resolution of 0.001  $\text{cm}^{-1}$ , using the same set-up described in detail in Refs. [35, 36], during a measurement campaign of the ND<sub>2</sub> radical. Although the experimental conditions were not optimized to form deuterated isotopologues of ammonia, the use of ND<sub>3</sub> as precursor in a radio-frequency discharge produced strong –but not saturating– lines of ND<sub>2</sub>H in the spectrum, as can be seen in Figure 1. Conversely, NH<sub>2</sub>D seems to be much less abundant and only a few absorption lines were detected; therefore, its FIR spectrum could not be analyzed.

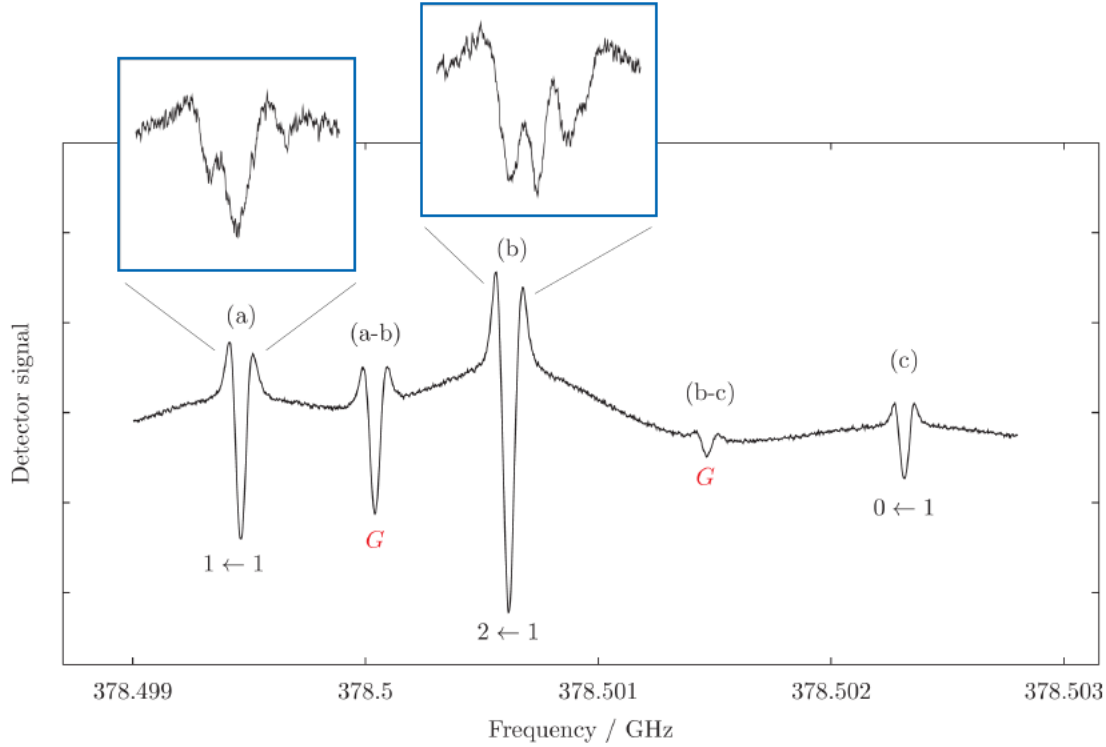


Figure 2: Lamb-dip spectrum of the  $J_{K_a, K_c} = 1_{1,0}^{(s)} - 0_{0,0}^{(a)}$   $p$ -ND<sub>2</sub>H transition. The numbers below each HFS components refer to the  $F'_1 \leftarrow F_1$  quantum numbers, while a red  $G$  indicates a ghost feature. The labels above each line are used to denote the “interacting” transition frequencies from which the ghost transitions arise. The magnified boxes show the splittings due to deuterium quadrupolar interaction, as observed at higher-resolution experimental conditions. The vertical scale of the plots represents the detector response in arbitrary units.

## 4. Results

### 4.1. Spectral analysis

The latest sets of spectroscopic constants for NH<sub>2</sub>D and ND<sub>2</sub>H were retrieved from Paper I and the Cologne Database for Molecular Spectroscopy (CDMS) [37], respectively. The quality of these parameters was sufficient to search and assign rotational transitions from the submillimeter-wave (submm) to the far-infrared domain. Moreover, in order to correctly interpret the hyperfine structure of the ND<sub>2</sub>H spectrum, the NQC, SR, and dipolar spin-spin (SS) tensors of doubly-deuterated ammonia were computed using the approach described in Paper I.

Briefly, the equilibrium values of the hyperfine constants were computed using the CCSD(T) method [38] in conjunction with a series of correlation-consistent  $n$ -uple-zeta basis sets [39, 40, 41, 42, 43] (with  $n = Q, 5, 6$ ), correlating all electrons, and extrapolated to the complete basis set (CBS) limit. Then, exploiting the additiv-

ity approximation [44], the contributions due to the full treatment of triple and quadruple excitations were also taken into account using triple- and double-zeta basis sets, respectively. Subsequently, the equilibrium hyperfine parameters were augmented by the corresponding vibrational corrections in order to estimate the vibrational ground-state values. These corrections have been evaluated within the second-order vibrational perturbation theory (VPT2) [45] at the CCSD(T)/aug-cc-pCVQZ level of theory (with all electrons correlated). All CCSD(T) computations have been performed using the CFOUR package [46, 47], while the MRCC program [48, 49] interfaced to CFOUR has been employed for CCSDT and CCSDTQ calculations. The computed values of all NQC, SR, and SS interaction constants are listed in Table 1. According to the literature on this topic (see, e.g., Refs. [27, 32, 50]), the computational methodology employed is able to provide quantitative predictions of hyperfine parameters. In more detail, for nuclear

quadrupole coupling constants, the discrepancy between experimental and computed values is below 20 kHz for parameters as small as those encountered in this work. Moving to nuclear spin-rotation constants, discrepancies usually range from hundredths of kHz to a few kHz.

Table 1: Computed nuclear quadrupole, spin-rotation, and dipolar spin-spin coupling constants of ND<sub>2</sub>H.

Constant	Atom	Unit	ND <sub>2</sub> H
$\chi_{aa}$	(N)	MHz	-2.048
$\chi_{cc}$	(N)	MHz	-3.842
$C_{aa}$	(N)	kHz	5.229
$C_{bb}$	(N)	kHz	3.756
$C_{cc}$	(N)	kHz	4.000
$\chi_{aa}$	(D)	MHz	0.135
$\chi_{cc}$	(D)	MHz	-0.124
$C_{aa}$	(D)	kHz	-1.228
$C_{bb}$	(D)	kHz	-1.888
$C_{cc}$	(D)	kHz	-1.860
$C_{aa}$	(H)	kHz	-23.595
$C_{bb}$	(H)	kHz	-5.058
$C_{cc}$	(H)	kHz	-9.115
$D_{bb}$	(N-D)	kHz	0.19
$D_{cc}$	(N-D)	kHz	0.98
$D_{bb}$	(N-H)	kHz	-8.62
$D_{cc}$	(N-H)	kHz	0.66
$D_{bb}$	(H-D)	kHz	-4.89
$D_{cc}$	(H-D)	kHz	3.82
$D_{bb}$	(D-D)	kHz	0.65
$D_{cc}$	(D-D)	kHz	0.65

**Notes:** The nuclear quadrupole ( $\chi_{ii}$ ) and dipolar spin-spin coupling ( $D_{ii}$ ) tensors have zero trace; therefore, only two of the three diagonal components are given.

For the first time, the complex hyperfine structure caused by the nitrogen and deuterium quadrupole couplings has been revealed in some low  $J$  transitions of ND<sub>2</sub>H. As an example, Figure 2 shows the Lamb-dip spectrum of the fundamental  $c$ -type rotation-inversion transition  $J_{K_a, K_c} = 1_{1,0}^{(s)} - 0_{0,0}^{(a)}$  of the *para* species. The main panel illus-

trates the three  $F_1$  components ( $\Delta F_1 = 0, \pm 1$ ) and two ghost transitions<sup>1</sup> (marked with a red  $G$ ) occurring in between, while the magnified boxes highlight the deuterium HF splittings corresponding to different  $F'_2 - F_2$  components. A similar resolution has been obtained also for the  $J_{K_a, K_c} = 1_{1,0}^{(a)} - 0_{0,0}^{(s)}$  transition of *o*-ND<sub>2</sub>H.

Additional measurements of NH<sub>2</sub>D and ND<sub>2</sub>H were performed with three main aims: (i) to resolve the HFS as much as possible for those transitions which can be used in astronomical observations (typically involving low-energy levels), (ii) to exploit the Lamb-dip technique at THz frequencies in order to achieve an accuracy of about 10 ppb on the line position, and (iii) to revise the submm and FIR spectra at higher resolution. In particular, we have observed about one hundred transitions of NH<sub>2</sub>D and ND<sub>2</sub>H in the mm/submm region, half of which show the HFS at least partially resolved. For ND<sub>2</sub>H only, we also detected and analyzed more than 700 distinct FIR transitions involving rotation-inversion levels with  $J$  up to 18.

The newly measured data were collected together with all pure-rotational literature data [51, 52, 53, 54, 55, 28, 27] and processed into a combined analysis. A least-squares procedure was performed with the SPFIT subroutine of the CALPGM program suite [56], where each datum is weighted proportionally to the inverse square of its uncertainty. The error associated to our line positions is in the range 2–100 kHz for mm/submm transitions and  $5 \times 10^{-5} \text{ cm}^{-1}$  for FIR lines, while literature data were used with their declared uncertainty. **Unresolved lines were incorporated in the fit as intensity-weighted average of the individual components involved in the blended feature, as implemented in SPFIT.**

The fit results for NH<sub>2</sub>D and ND<sub>2</sub>H have similar quality, despite the different number of available data. The overall fit standard deviation ( $\sigma$ ) is close to 1 in both cases and the root-mean-square (rms) error is below 100 kHz for mm/submm data and around  $0.0002 \text{ cm}^{-1}$  for the FIR transitions. These values indicate that the modeling of both species is satisfactory and can be used to generate spectral predictions in a wide range of frequencies

<sup>1</sup>Ghost transitions, also denoted as crossover resonances, are due to the saturation of overlapping Gaussian profiles of two transitions sharing a common energy level. They occur at the arithmetic mean frequency of the overlapping transitions.



with a low uncertainty. The derived rotational and centrifugal distortion constants, Coriolis interaction terms, and HFS parameters are given in Tables 2–4. All parameters have been improved, with respect to previous studies, by up to one order of magnitude. Moreover, the ND<sub>2</sub>H quadrupole coupling constant  $\chi_{cc}(\text{D})$  has been determined for the first time and allows the simulation of the deuterium HFS. Its derived value, -0.121(4), agrees very well with the computed counterpart, -0.124. Instead, the hydrogen HFS could not be resolved in the laboratory spectra, thus preventing the experimental determination of the hydrogen spin-rotation constants. Simulations based on the calculated parameters showed that the hydrogen HFS is so small that it does not affect the spectral linewidths.

The SPFIT input files (.PAR and .LIN) as well as a re-formatted version of the .FIT output file are provided for both species as Supplementary Material.

#### 4.2. Line catalogs for astronomical purposes

In order to produce meaningful line lists that can be used for astronomical observations of NH<sub>2</sub>D and ND<sub>2</sub>H, the new sets of spectroscopic constants must be combined with accurate estimates of the rotational partition function ( $Q_{\text{rot}}$ ) and dipole moment components. The latter were evaluated in Refs. [54] and [28] and are:  $\mu_a = -0.185$  D and  $\mu_c = 1.46$  D for NH<sub>2</sub>D and  $\mu_b = 0.21$  D and  $\mu_c = 1.47$  D for ND<sub>2</sub>H.

The rotational partition functions, instead, have been calculated numerically using the SPCAT subroutine of the CALPGM suite [56]. The temperature dependence of  $Q_{\text{rot}}$  was computed separately for the *ortho* and *para* species at three different “resolutions”: (i) without the inclusion of any HFS, (ii) considering only the contribution of nitrogen, and (iii) including the effects of both N and D nuclei. These distinctions have been made in order to support the analysis of interstellar deuterated ammonia at different spectral resolution. Moreover, at the low temperatures of cold molecular clouds (5–10 K), the *ortho* and *para* species must be treated as separate species. The rotational partition function values computed at temperatures between 2.725 and 300 K are provided as Supplementary Material.

#### 4.3. Application to L1544 starless core spectrum

To test the effect of the inclusion of D hyperfine structure in the analysis of astrophysical NH<sub>2</sub>D

Table 2: Ground-state rotational and centrifugal distortion constants up to the sixth power of the angular momentum.

Constant <sup>(a)</sup>	Unit	NH <sub>2</sub> D	ND <sub>2</sub> H
$\Delta E$	MHz	12169.466(1)	5118.8865(8)
$A$	MHz	290074.6(2)	223187.715(1)
$\Delta A$	MHz	-46.9120(8)	-16.1290(6)
$B$	MHz	192176.4768(8)	160214.998(4)
$\Delta B$	MHz	-17.34(2)	-5.3284(4)
$C$	MHz	140810.2(2)	112520.741(4)
$\Delta C$	MHz	11.2003(1)	4.0868(4)
$D_J$	MHz	15.7199(1)	3.5183(2)
$\Delta D_J$	MHz	-0.09412(4)	-0.000896(5)
$D_{JK}$	MHz	-23.7516(2)	-2.9356(9)
$\Delta D_{JK}$	MHz	0.19484(9)	-0.01008(3)
$D_K$	MHz	10.8484(3)	19.2808(7)
$\Delta D_K$	MHz	-0.10982(6)	-0.04472(5)
$d_1$	MHz	4.14089(8)	-1.2318(2)
$\Delta d_1$	MHz	-0.04166(4)	0.000795(4)
$d_2$	MHz	0.13787(4)	-0.28029(7)
$\Delta d_2$	MHz	0.00567(3)	0.001787(2)
$H_J$	kHz	3.537(3)	0.3353(9)
$\Delta H_J$	kHz	-0.1940(5)	0.00160(5)
$H_{JK}$	kHz	-8.422(4)	-1.21(1)
$\Delta H_{JK}$	kHz	0.4048(8)	-0.0055(2)
$H_{KJ}$	kHz	8.776(7)	2.16(4)
$\Delta H_{KJ}$	kHz	-0.3824(9)	-0.049(1)
$H_K$	kHz	-3.705(8)	4.75(3)
$\Delta H_K$	kHz	0.1762(4)	-0.089(1)
$h_1$	kHz	-1.832(3)	0.247(1)
$\Delta h_1$	kHz	0.1097(6)	-0.00060(3)
$h_2$	kHz	0.445(2)	0.0382(5)
$\Delta h_2$	kHz	-0.0146(6)	-0.00160(2)
$h_3$	kHz	-0.0403(5)	0.0225(2)
$\Delta h_3$	Hz	-0.0086(3)	-0.00097(1)

**Notes:** Numbers in parentheses are standard errors and apply to the last significant digits. <sup>(a)</sup> For a given parameter  $X$ ,  $\Delta X = (X^{(a)} - X^{(s)})/2$ .

emissions at millimeter wavelengths, we have used recent observations of the starless core L1544, a low-mass star-forming core in a very early stage of evolution. This source is a prototypical cold, quiescent core on the verge of the gravitational collapse, which exhibits very narrow line emissions due its low central temperature, subsonic contraction motion, and low turbulence [57, 58]. It also shows a high degree of deuteration [e.g., Ref. 59]) which



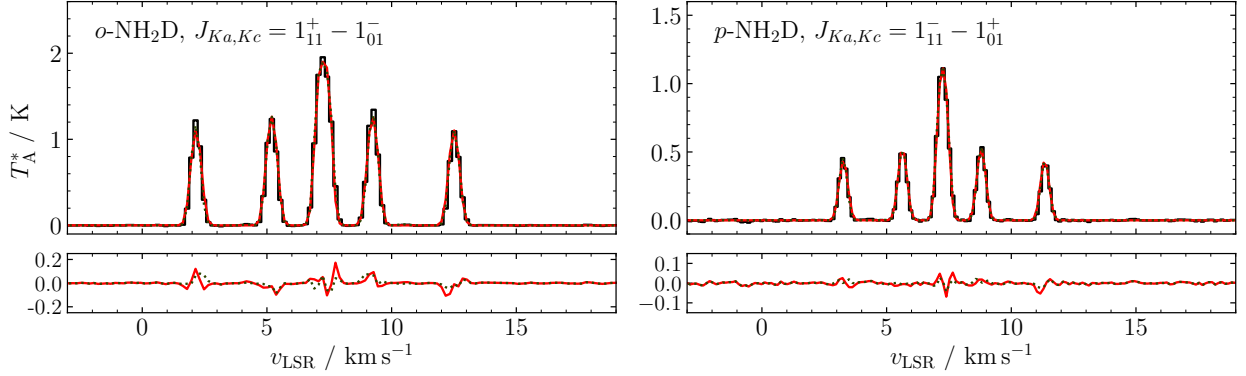


Figure 3: Spectra of the NH<sub>2</sub>D transitions observed towards L1544. (*Top left panel*):  $J_{K_a, K_c} = 1_{1,1}^{(s)} - 1_{0,1}^{(a)}$  *ortho* line at 85926.3 MHz. (*Top right panel*):  $J_{K_a, K_c} = 1_{1,1}^{(a)} - 1_{0,1}^{(s)}$  *para* line at 110153.6 MHz. The dotted green trace plots the model computed considering the full HFS (N+D). The solid red trace plots the model computed with the N quadrupole only. (*Bottom panels*): Residuals of both models, plotted using the same colour legend.

makes it an ideal astrophysical laboratory to observe D-containing molecules and to reveal subtle spectral effects due to the contribution of the deuterium quadrupole splittings.

The astronomical data used here were collected using the IRAM 30m telescope (Pico Veleta, Spain) in the past few years by some members of our team. They were observed as part of the projects 008-12, 013-13 (PI S. Spezzano) and 150-11, 127-12 (PI L. Bizzocchi). The observing runs were performed in several sessions from May 2012 to October 2013. The frequency intervals of interest have been extracted from the output of the wide-band FTS spectrometer which was connected to the 3 mm band of the EMIR heterodyne receiver. The *o*-NH<sub>2</sub>D lines at 85926.3 MHz and the ones of *p*-NH<sub>2</sub>D at 110153.6 MHz were observed in the lower-outer (LO) and upper-inner (UI) sub-band, respectively. A detailed description of the observation strategy and the data reduction can be found elsewhere [60, 61, 62].

The resulting spectra are shown in the two panels of Figure 3, plotted as black histograms. Note that the *x*-axis is labelled in radial equivalent velocity using the rest frequency of the corresponding unsplit lines as reference. The solid red lines plot the best fit model computed using the full HFS (including D). The fitting was performed using a custom Python3 code described in Ref. [12]. The free parameters of the optimisation are the column density (*N*), the excitation temperature ( $T_{\text{ex}}$ ), the systemic velocity ( $v_{\text{LSR}}$ ) and the line full-width-half-maximum (FWHM), while the total opacity of the

transition ( $\tau$ ) is regarded as a derived quantity.

Table 5 collects the fit results of two different analyses obtained by taking into account the nitrogen quadrupole coupling only (column labelled by N) or the full hyperfine structure including the deuterium effects (N+D). While the two models would be virtually indistinguishable by visual inspection, small but significant differences are highlighted by the fit results. Apart from a 30-40% reduction of the residual rms, the proper treatment of the hyperfine effects entails a reduction of the derived line FWHM of about 12%. This change is reflected by the values of the related parameter *N* and  $T_{\text{ex}}$ , and of the derived quantity  $\tau$ . For the less opaque emission (*p*-NH<sub>2</sub>D), the column density and the excitation temperature readjust, while  $\tau$  remains substantially unchanged. For the thicker *o*-NH<sub>2</sub>D line, the  $T_{\text{ex}}$  is unaffected and the deviation is mainly observed by a relevant change of  $\tau$ .

## 5. Conclusions

The rotational spectra of singly- and doubly-deuterated ammonia have been thoroughly re-investigated at higher resolution. By means of the Lamb-dip technique at submillimeter wavelengths and with the use of synchrotron radiation in the FIR region, a large number of transitions have been measured with high accuracy. For some of them, the nitrogen and deuterium hyperfine structure due to electric and magnetic interactions has been unveiled, thus allowing the precise determination of

Table 3: Higher-order centrifugal distortion constants and Coriolis interaction parameters.

Constant <sup>(a)</sup>	Unit	NH <sub>2</sub> D	ND <sub>2</sub> H
$L_J$	Hz	-1.14(2)	
$\Delta L_J$	mHz	181.(2)	-3.7(1)
$L_{JJK}$	Hz	3.27(2)	-0.123(5)
$\Delta L_{JJK}$	Hz	-0.468(5)	
$L_{JK}$	Hz	-5.63(7)	-0.50(4)
$\Delta L_{JK}$	Hz	0.711(8)	
$L_{KKJ}$	Hz	5.1(1)	1.4(1)
$\Delta L_{KKJ}$	Hz	-0.729(6)	0.30(1)
$L_K$	Hz	-2.1(1)	-3.60(6)
$\Delta L_K$	Hz	0.306(2)	-0.026(6)
$l_1$	Hz	0.80(2)	0.080(3)
$\Delta l_1$	mHz	-22.(2)	0.38(5)
$l_2$	Hz	-0.30(1)	-0.0185(3)
$\Delta l_2$	mHz	-152.(6)	1.98(6)
$l_3$	mHz	18.(3)	-4.7(2)
$\Delta l_3$	mHz	112.(5)	0.14(5)
$l_4$	mHz		-1.55(6)
$\Delta l_4$	mHz	-22.(1)	0.48(1)
$M_{KKJ}$	mHz		1.35(3)
$M_K$	mHz	1.3(3)	1.35(3)
$F_{ij}$	MHz	-5097.(3)	3129.49(4)
$F_{ij}^J$	MHz		0.812(3)
$F_{ij}^K$	MHz		-9.00(2)
$F_{ij}^{JJ}$	kHz		-1.49(2)
$F_{ij}^{JK}$	kHz		4.4(1)
$F_{ij}^{KK}$	kHz		9.8(4)
$F_{ij}^{JJJ}$	Hz		-1.22(4)

**Notes:** Numbers in parentheses are standard errors and apply to the last significant digits. <sup>(a)</sup> For a given parameter  $X$ ,  $\Delta X = (X^{(a)} - X^{(s)})/2$ .  $F_{ij}$  corresponds to  $F_{ab}$  and  $F_{bc}$  for NH<sub>2</sub>D and ND<sub>2</sub>H, respectively.

nuclear quadrupole coupling and spin-rotation constants. Moreover, all the values of rotational and centrifugal distortion parameters could be refined thanks to the analysis of an extended dataset.

The new set of spectroscopic constants has been then used to evaluate the impact of the deuterium HFS on the analysis of astrophysical NH<sub>2</sub>D lines towards L1544. The narrow line emissions of this pre-stellar core made it possible to detect small but significant differences in the physical parameters determined when both nitrogen and deuterium hyperfine interactions are taken into account. In addition

Table 4: Nitrogen and deuterium hyperfine constants (only the parameters used in the analyses are listed).

Constant	Atom	Unit	NH <sub>2</sub> D	ND <sub>2</sub> H
$\chi_{aa}$	(N)	MHz	1.909(3)	-2.038(8)
$\chi_{cc}$	(N)	MHz	-3.948(1)	-3.852(2)
$C_{aa}$	(N)	kHz	6.1(8)	5.229
$C_{bb}$	(N)	kHz	3.8(7)	3.756
$C_{cc}$	(N)	kHz	5.1(2)	4.000
$\chi_{aa}$	(D)	MHz	0.225(5)	0.132
$\chi_{cc}$	(D)	MHz	-0.135(1)	-0.121(4)
$C_{aa}$	(D)	kHz	-0.125	-1.228
$C_{bb}$	(D)	kHz	-3.154	-1.888
$C_{cc}$	(D)	kHz	-2.27(9)	-1.860

**Notes:** Numbers within parentheses are the standard errors and apply to the last significant digits. Non-determinable parameters (values given without error) have been kept fixed at the corresponding computed values (see Table 1).

to the improvement of the fit results in term of rms residual, the observed reduction of the line FWHM produces a change in the determination of the column density of *ortho*- and *para*-NH<sub>2</sub>D of about 5–20 %. This observation demonstrates the importance of modelling all the effects that can contribute to the determination of molecular abundances for interstellar species.

## 6. Supplementary Material Available

The file “partition-function-values.pdf” contains the rotational partition function values computed at temperatures between 2.725 and 300 K for the *ortho* and *para* species of ND<sub>2</sub>H and NH<sub>2</sub>D. The files “nh2d.lin”, “nh2d.par”, “nd2h.lin”, and “nd2h.par” are the SPFIT input files used in our analysis. The files “nh2d\_reformatted.out” and “nd2h\_reformatted.out” are a reformatted version of the SPFIT output files.

## 7. Acknowledgement

This study was supported by Bologna University (RFO funds) and by MIUR (Project PRIN 2015: STARS in the CAOS, Grant Number 2015F59J3R), and in Mainz by the Deutsche Forschungsgemeinschaft via grant GA 370/6-2. Part of the measurements has been performed under the SOLEIL

Table 5: Analysis of the ortho and para NH<sub>2</sub>D emissions in L1544 considering nitrogen quadrupole coupling only (N) or the full hyperfine structure (N+D).

Parameter	Unit	<i>o</i> -NH <sub>2</sub> D		<i>p</i> -NH <sub>2</sub> D	
		N	N+D	N	N+D
$N$	$10^{14} \text{ cm}^{-2}$	5.92(20)	5.64(15)	3.01(14)	2.44(9)
$T_{\text{ex}}$	K	4.46(2)	4.47(2)	3.95(3)	4.07(2)
$v_{\text{LSR}}$	$\text{km s}^{-1}$	7.265(2)	7.265(2)	7.194(1)	7.195(1)
FWHM	$\text{km s}^{-1}$	0.444(3)	0.388(3)	0.389(3)	0.346(2)
$\tau^a$		7.47	8.22	3.48	3.46
rms <sup>b</sup>	mK	56	39	19	11

**Notes:** Numbers within parentheses are the standard errors and apply to the last significant digits. <sup>a</sup> Derived quantity. <sup>b</sup> Root-mean-square of the residuals computed on lines.

proposal #20110017; we acknowledge the SOLEIL facility for provision of synchrotron radiation and would like to thank the AILES beamline staff for their assistance and in particular Dr. M.-A. Martin-Drumel and Dr. O. Pirali for their help during the spectral recording. L.B., S.S. and P.C. acknowledge the support by the Max Planck Society. N.J. thanks the China Scholarships Council (CSC) for the financial support.

## References

- [1] B. A. McGuire, 2018 Census of Interstellar, Circumstellar, Extragalactic, Protoplanetary Disk, and Exoplanetary Molecules, *Astrophys. J. Suppl. S.* 239 (2018) 17.
- [2] A. López-Sepulcre, N. Balucani, C. Ceccarelli, C. Codella, F. Dulieu, P. Theulé, Interstellar formamide (NH<sub>2</sub>CHO), a key prebiotic precursor, *ACS Earth Space Chem.* 3 (10) (2019) 2122–2137.
- [3] V. M. Rivilla, J. Martín-Pintado, I. Jiménez-Serra, S. Martín, L. F. Rodríguez-Almeida, M. A. Requena-Torres, et al., Prebiotic precursors of the primordial RNA world in space: Detection of NH<sub>2</sub>OH, *Astrophys. J. Lett.* 899 (2) (2020) L28.
- [4] S. A. Sandford, M. Nuevo, P. P. Bera, T. J. Lee, Prebiotic astrochemistry and the formation of molecules of astrobiological interest in interstellar clouds and protostellar disks, *Chem. Rev.*
- [5] Y.-J. Kuan, S. B. Charnley, H.-C. Huang, W.-L. Tseng, Z. Kisiel, Interstellar glycine, *Astrophys. J.* 593 (2) (2003) 848.
- [6] L. E. Snyder, F. J. Lovas, J. M. Hollis, D. N. Friedel, P. R. Jewell, A. Remijan, et al., A rigorous attempt to verify interstellar glycine, *Astrophys. J.* 619 (2) (2005) 914–930. doi:10.1086/426677. URL <https://doi.org/10.1086/426677>
- [7] M. Melosso, B. A. McGuire, F. Tamassia, C. Degli Esposti, L. Dore, Astronomical search of vinyl alcohol assisted by submillimeter spectroscopy, *ACS Earth and Space Chemistry* 3 (7) (2019) 1189–1195.
- [8] M. Melosso, L. Dore, F. Tamassia, C. L. Brogan, T. R. Hunter, B. A. McGuire, The sub-millimeter rotational spectrum of ethylene glycol up to 890 GHz and application to ALMA Band 10 spectral line data of NGC 6334I, *J. Phys. Chem. A* 124 (2020) 240–246.
- [9] A. Belloche, R. Garrod, H. Müller, K. Menten, I. Medvedev, J. Thomas, Z. Kisiel, Re-exploring Molecular Complexity with ALMA (ReMoCA): interstellar detection of urea, *Astron. Astrophys.* 628 (2019) A10.
- [10] E. R. Alonso, B. A. McGuire, L. Kolesníková, P. B. Carroll, I. León, C. L. Brogan, et al., The laboratory millimeter and submillimeter rotational spectrum of lactaldehyde and an astronomical search in Sgr B2 (N), Orion-KL, and NGC 6334I, *Astrophys. J.* 883 (1) (2019) 18.
- [11] R. Güsten, H. Wiesemeyer, D. Neufeld, K. M. Menten, U. U. Graf, K. Jacobs, et al., Astrophysical detection of the helium hydride ion HeH<sup>+</sup>, *Nature* 568 (7752) (2019) 357–359.
- [12] M. Melosso, L. Bizzocchi, O. Sipilä, B. Giuliano, L. Dore, F. Tamassia, et al., First detection of NHD and ND<sub>2</sub> in the interstellar medium. amidogen deuteration in IRAS 16293–2422, *Astron. Astrophys.* 641 (2020) A153.
- [13] J. Cernicharo, N. Marcelino, J. Pardo, M. Agúndez, B. Tercero, P. de Vicente, et al., Interstellar nitrile anions: Detection of C<sub>3</sub>N<sup>−</sup> and C<sub>5</sub>N<sup>−</sup> in TMC-1, *Astron. Astrophys.* 641 (2020) L9.
- [14] R. A. Loomis, A. M. Burkhardt, C. N. Shingledecker, S. B. Charnley, M. A. Cordiner, E. Herbst, et al., An investigation of spectral line stacking techniques and application to the detection of HC<sub>11</sub>N, *Nat. Astron.* [arXiv:2009.11900](https://arxiv.org/abs/2009.11900), doi:10.1086/523645.
- [15] M. C. McCarthy, K. L. K. Lee, R. A. Loomis, A. M. Burkhardt, C. N. Shingledecker, S. B. Charnley, et al., Interstellar detection of the highly polar five-membered ring cyanocyclopentadiene, *Nat. Astron.* (2020) 1–5.
- [16] B. A. McGuire, A. M. Burkhardt, S. Kalenskii, C. N. Shingledecker, A. J. Remijan, E. Herbst, M. C. Mc-

- Carthy, Detection of the aromatic molecule benzonitrile ( $c\text{-C}_6\text{H}_5\text{CN}$ ) in the interstellar medium, *Science* 359 (6372) (2018) 202–205.
- [17] A. Coletta, F. Fontani, V. Rivilla, C. Mininni, L. Colzi, Á. Sánchez-Monge, M. Beltrán, Evolutionary study of complex organic molecules in high-mass star-forming regions, *Astron. Astrophys.* 641 (2020) A54.
- [18] J. K. Jørgensen, A. Belloche, R. T. Garrod, Astrochemistry during the formation of stars, *Ann. Rev. Astron. Astrophys.* 58 (2020) 727–778.
- [19] P. Caselli, T. Hasegawa, E. Herbst, Chemical differentiation between star-forming regions—the Orion hot core and compact ridge, *Astrophys. J.* 408 (1993) 548–558.
- [20] S. Spezzano, L. Bizzocchi, P. Caselli, J. Harju, S. Brünken, Chemical differentiation in a prestellar core traces non-uniform illumination, *Astron. Astrophys.* 592 (2016) L11.
- [21] Y. Aikawa, K. Furuya, S. Yamamoto, N. Sakai, Chemical variation among protostellar cores: Dependence on prestellar core conditions, *Astrophys. J.* 897 (2) (2020) 110.
- [22] L. Bizzocchi, F. Tamassia, J. Laas, B. M. Giuliano, C. Degli Esposti, L. Dore, et al., Rotational and high-resolution infrared spectrum of  $\text{HC}_3\text{N}$ : global ro-vibrational analysis and improved line catalog for astrophysical observations, *Astrophys. J. Suppl. S.* 233 (1) (2017) 11.
- [23] M. Melosso, A. Belloche, M.-A. Martin-Drumel, O. Pirali, F. Tamassia, L. Bizzocchi, et al., Far-infrared laboratory spectroscopy of aminoacetonitrile and first interstellar detection of its vibrationally excited transitions, *Astron. Astrophys.* 641 (2020) A160.
- [24] M. Carvajal, C. Favre, I. Kleiner, C. Ceccarelli, E. Bergin, D. Fedele, Impact of nonconvergence and various approximations of the partition function on the molecular column densities in the interstellar medium, *Astron. Astrophys.* 627 (2019) A65.
- [25] F. Daniel, L. Coudert, A. Puanova, J. Harju, A. Faure, E. Roueff, et al., The  $\text{NH}_2\text{D}$  hyperfine structure revealed by astrophysical observations, *Astron. Astrophys.* 586 (2016) L4.
- [26] J. Harju, F. Daniel, O. Sipilä, P. Caselli, J. E. Pineda, R. K. Friesen, et al., Deuteration of ammonia in the starless core Ophiuchus/H-MM1, *Astron. Astrophys.* 600 (2017) A61.
- [27] M. Melosso, L. Dore, J. Gauss, C. Puzzarini, Deuterium hyperfine splittings in the rotational spectrum of  $\text{NH}_2\text{D}$  as revealed by Lamb-dip spectroscopy, *J. Mol. Spectrosc.* (2020) 111291.
- [28] C. Endres, H. Müller, S. Brünken, D. Paveliev, T. Giesen, S. Schlemmer, F. Lewen, High resolution rotation-inversion spectroscopy on doubly deuterated ammonia,  $\text{ND}_2\text{H}$ , up to 2.6 THz, *J. Mol. Struct.* 795 (1–3) (2006) 242–255.
- [29] M. Melosso, L. Bizzocchi, F. Tamassia, C. Degli Esposti, E. Cané, L. Dore, The rotational spectrum of  $^{15}\text{ND}$ . isotopic-independent Dunham-type analysis of the imidogen radical, *Phys. Chem. Chem. Phys.* 21 (2019) 3564–3573.
- [30] M. Melosso, C. Degli Esposti, L. Dore, Terahertz spectroscopy and global analysis of the rotational spectrum of doubly deuterated amidogen radical  $\text{ND}_2$ , *Astrophys. J. Suppl. S.* 233 (1) (2017) 15.
- [31] M. Melosso, B. Conversazioni, C. Degli Esposti, L. Dore, E. Cané, F. Tamassia, L. Bizzocchi, The pure rotational spectrum of  $^{15}\text{ND}_2$  observed by millimetre and submillimetre-wave spectroscopy, *J. Quant. Spectrosc. Ra.* 222 (2019) 186–189.
- [32] C. Puzzarini, G. Cazzoli, M. E. Harding, J. Vázquez, J. Gauss, A new experimental absolute nuclear magnetic shielding scale for oxygen based on the rotational hyperfine structure of  $\text{H}^{17}_2\text{O}$ , *J. Chem. Phys.* 131 (2009) 234304.
- [33] C. Puzzarini, G. Cazzoli, M. E. Harding, J. Vázquez, J. Gauss, The hyperfine structure in the rotational spectra of  $\text{D}^{17}_2\text{O}$  and  $\text{HD}^{17}\text{O}$ : Confirmation of the absolute nuclear magnetic shielding scale for oxygen, *J. Chem. Phys.* 142 (2015) 124308.
- [34] L. Dore, L. Bizzocchi, C. Degli Esposti, J. Gauss, The magnetic hyperfine structure in the rotational spectrum of  $\text{H}_2\text{CNH}$ , *J. Mol. Spectrosc.* 263 (2010) 44–50.
- [35] L. Bizzocchi, M. Melosso, B. M. Giuliano, L. Dore, F. Tamassia, M.-A. Martin-Drumel, et al., Submillimeter and far-infrared spectroscopy of monodeuterated amidogen radical (NHD): Improved rest frequencies for astrophysical observations, *Astrophys. J. Suppl. S.* 247 (2) (2020) 59.
- [36] M. Melosso, L. Bizzocchi, A. Adamczyk, E. Cané, P. Caselli, L. Colzi, et al., Extensive ro-vibrational analysis of deuterated-cyanoacetylene ( $\text{DC}_3\text{N}$ ) from millimeter-wavelengths to the infrared domain, *J. Quant. Spectrosc. Ra.* 254 (2020) 107221.
- [37] H. S. Müller, F. Schlöder, J. Stutzki, G. Winnewisser, The Cologne database for molecular spectroscopy, CDMS: a useful tool for astronomers and spectroscopists, *J. Mol. Struct.* 742 (1–3) (2005) 215–227.
- [38] K. Raghavachari, G. W. Trucks, J. A. Pople, M. Head-Gordon, A fifth-order perturbation comparison of electron correlation theories, *Chem. Phys. Lett.* 157 (1989) 479–483.
- [39] T. H. Dunning Jr., Gaussian Basis Sets for Use in Correlated Molecular Calculations. I. The Atoms Boron through Neon and Hydrogen, *J. Chem. Phys.* 90 (1989) 1007.
- [40] A. Kendall, T. H. Dunning Jr., R. J. Harrison, Electron affinities of the first-row atoms revisited. Systematic basis sets and wave functions, *J. Chem. Phys.* 96 (1992) 6796.
- [41] D. E. Woon, T. H. Dunning Jr., Gaussian basis sets for use in correlated molecular calculations. V. Core-valence basis sets for boron through neon, *J. Chem. Phys.* 103 (1995) 4572.
- [42] A. K. Wilson, T. van Mourik, T. H. Dunning Jr, Gaussian basis sets for use in correlated molecular calculations. VI. Sextuple zeta correlation consistent basis sets for boron through neon, *J. Mol. Struct. THEOCHEM* 388 (1996) 339–349.
- [43] T. Van Mourik, A. K. Wilson, T. H. Dunning Jr, Benchmark calculations with correlated molecular wavefunctions. XIII. Potential energy curves for  $\text{He}_2$ ,  $\text{Ne}_2$  and  $\text{Ar}_2$  using correlation consistent basis sets through augmented sextuple zeta, *Mol. Phys.* 96 (1999) 529–547.
- [44] C. Puzzarini, M. Heckert, J. Gauss, The accuracy of rotational constants predicted by high-level quantum-chemical calculations. i. molecules containing first-row atoms, *J. Chem. Phys.* 128 (19) (2008) 194108.
- [45] I. M. Mills, Vibration-rotation structure in asymmetric and symmetric-top molecules, Vol. 1, 1972, p. 115.
- [46] J. F. Stanton, J. Gauss, L. Cheng, M. E. Harding, D. A. Matthews, P. G. Szalay, CFOUR, coupled-cluster

- techniques for computational chemistry, a quantum-chemical program package, With contributions from A.A. Auer, R.J. Bartlett, U. Benedikt, C. Berger, D.E. Bernholdt, Y.J. Bomble, O. Christiansen, F. Engel, R. Faber, M. Heckert, O. Heun, M. Hilgenberg, C. Huber, T.-C. Jagau, D. Jonsson, J. Jusélius, T. Kirsch, K. Klein, W.J. Lauderdale, F. Lipparini, T. Metzroth, L.A. Mück, D.P. O'Neill, D.R. Price, E. Prochnow, C. Puzzarini, K. Ruud, F. Schiffmann, W. Schwalbach, C. Simmons, S. Stopkowitz, A. Tajti, J. Vázquez, F. Wang, J.D. Watts and the integral packages MOLECULE (J. Almlöf and P.R. Taylor), PROPS (P.R. Taylor), ABACUS (T. Helgaker, H.J. Aa. Jensen, P. Jørgensen, and J. Olsen), and ECP routines by A. V. Mitin and C. van Wüllen. For the current version, see <http://www.cfour.de>.
- [47] D. A. Matthews, L. Cheng, M. E. Harding, F. Lipparini, S. Stopkowitz, T.-C. Jagau, et al., Coupled-cluster techniques for computational chemistry: The cfour program package, *J. Chem. Phys.* 152 (21) (2020) 214108.
- [48] M. Kállay, MRCC, a generalized CC/CI program, For the current version, see <http://www.mrcc.hu>.
- [49] M. Kállay, P. R. Nagy, D. Mester, Z. Rolik, G. Samu, J. Csontos, et al., The mrcc program system: Accurate quantum chemistry from water to proteins, *J. Chem. Phys.* 152 (7) (2020) 074107.
- [50] T. Helgaker, J. Gauss, G. Cazzoli, C. Puzzarini,  $^{33}\text{S}$  hyperfine interactions in  $\text{H}_2\text{S}$  and  $\text{SO}_2$  and revision of the sulfur nuclear magnetic shielding scale, *J. Chem. Phys.* 139 (2013) 244308.
- [51] M. Weiss, M. W. P. Strandberg, The microwave spectra of the deuterio-ammonias, *Phys. Rev.* 83 (1951) 567.
- [52] M. Lichtenstein, J. Gallagher, V. Derr, Spectroscopic investigations of the deuterio-ammonias in the millimeter region, *J. Mol. Spectrosc.* 12 (1) (1964) 87–97.
- [53] F. C. De Lucia, P. Helminger, Millimeter-and submillimeter-wave length spectrum of the partially deuterated ammonias; a study of inversion, centrifugal distortion, and rotation-inversion interactions, *J. Mol. Spectrosc.* 54 (1975) 200–214.
- [54] E. Cohen, H. Pickett, The rotation-inversion spectra and vibration-rotation interaction in  $\text{NH}_2\text{D}$ , *J. Mol. Spectrosc.* 93 (1982) 83–100.
- [55] L. Fusina, G. Di Leonardo, J. Johns, L. Halonen, Far-infrared spectra and spectroscopic parameters of  $\text{NH}_2\text{D}$  and  $\text{ND}_2\text{H}$  in the ground state, *J. Mol. Spectrosc.* 127 (1988) 240–254.
- [56] H. M. Pickett, The fitting and prediction of vibration-rotation spectra with spin interactions, *J. Mol. Spectrosc.* 148 (1991) 371–377.
- [57] M. Tafalla, P. Myers, P. Caselli, C. Walmsley, C. Comito, Systematic molecular differentiation in starless cores, *Astrophys. J.* 569 (2) (2002) 815.
- [58] E. Keto, P. Caselli, Dynamics and depletion in thermally supercritical starless cores, *Mon. Not. R. Astron. Soc.* 402 (3) (2010) 1625–1634.
- [59] E. Redaelli, L. Bizzocchi, P. Caselli, O. Sipilä, V. Latanzi, B. Giuliano, S. Spezzano, High-sensitivity maps of molecular ions in l1544-i. deuteration of  $\text{n}_2\text{h}^+$  and  $\text{hco}^+$  and primary evidence of  $\text{n}_2\text{d}^+$  depletion, *Astron. Astrophys.* 629 (2019) A15.
- [60] S. Spezzano, S. Brünken, P. Schilke, P. Caselli, K. Menten, M. McCarthy, et al., Interstellar detection of  $\text{c-C}_3\text{D}_2$ , *Astrophys. J. Lett.* 769 (2) (2013) L19.
- [61] S. Spezzano, H. Gupta, S. Brünken, C. Gottlieb, P. Caselli, K. Menten, et al., A study of the  $\text{C}_3\text{H}_2$  isomers and isotopologues: first interstellar detection of HDCCC, *Astron. Astrophys.* 586 (2016) A110.
- [62] L. Bizzocchi, P. Caselli, S. Spezzano, E. Leonardo, Deuterated methanol in the pre-stellar core L1544, *Astron. Astrophys.* 569 (2014) A27.